CHEMISTRY
A EUROPEAN JOURNAL

DOI: 10.1002/chem.200500835

Complex Wurtzite ZnSe Microspheres with High Hierarchy and Their Optical Properties

Weitang Yao, Shu-Hong Yu,* Jun Jiang, and Lin Zhang[a]

Abstract: Complex wurtzite ZnSe microspheres with hierarchical fractal structure and showing strong quantum-size effects can be prepared easily by a mild solvothermal reaction in a diethylenetriamine (DETA)–deionized water (DIW) binary solution. The ZnSe microspheres are made up of nanosheets, each formed by the face-to-face pairing of two individual nanosheets. In addition, high-order, flowerlike hierarchical structures are formed by the attachment of flexible, uniform nanofibers to the exposed faces of each nanosheet pair. The surface morphology of the nanosheets changed as reaction time increased and the detailed phase-transformation and shape-evolution processes were studied. This approach could provide an effective strategy for tuning the electronic and optical properties of semiconductors, with special advantages over the traditional high-temperature approach, and could be extended to access other semiconductor materials with unusual morphologies and structures.

Keywords: microspheres · nanostructures · photoluminescence · selenium · semiconductors · zinc

Introduction

The landmark discovery of the first blue-emitting laser diodes based on zinc selenide led to further development of zinc selenide as an optoelectronic material.[1] As one of the Zn-based II–VI compounds, ZnSe is a direct band-gap semiconductor, with a room-temperature band-gap energy and an emission at 2.7 eV, suggesting it to be a potentially good material for blue-diode lasers and other photoelectronic devices.[2–5] Therefore, ZnSe is of great interest as a model material for thin films,[6] quantum wells or qutantum dots,[7] bulk crystals,[8] and ZnSe-based optoelectronic devices.[9]

Stimulated by the novel properties of ZnSe, various morphologies of ZnSe nanostructures have been synthesized by diverse methods and various synthesizing systems, which are expected to offer new opportunities for applications in emerging fields of nanoscience and nanotechnology. Several ZnSe low-dimensional nanostructures, such as nanocrystals,[5,10] nanorods,[11] nanowires and nanoribbons,[12] and monodispersed ZnSe microspheres[13] have been reported. Diamines have also been used for the synthesis of semiconductor nanoparticles[14] and organic–inorganic hybrid structures containing two-dimensional II–VI slabs, such as $ZnSe(en)_{0.5}$ and $ZnTe(en)_{0.5}$, which often act as intermediates for the synthesis of II–VI nanoparticles.[15–17] Recently, we synthesized flexible wurtzite-type ZnS nanobelts by using a solvothermal approach and a diamine/water binary solution.[18] We also synthesized an inorganic–organic hybrid semiconductor nanobelt $[ZnSe](DETA)_{0.5}$ (DETA = diethylenetriamine) in ternary solution.[19]

Here, we report a controllable solution strategy for the synthesis in a binary solution of a new kind of wurtzite ZnSe microsphere with complex structure. These novel microspheres with fractal structures were formed by branched nanosheets. Each nanosheet is composed of twinned nanosheets, with ZnSe nanofibers attached to the exposed, nonfacing nanosheet surfaces. We investigated the effects of reaction conditions on the formation and phase evolution of these structures, as well as their optical properties.

Results and Discussion

Time-dependent phase transformation: The composition of the product is strongly dependent on reaction time. Figure 1

[a] Dr. W. Yao, Prof. Dr. S.-H. Yu, J. Jiang, L. Zhang
Division of Nanomaterials and Chemistry
Hefei National Laboratory for Physical Sciences at Microscale
Structure Research Laboratory of CAS
School of Chemistry and Materials
University of Science and Technology of China
Hefei, Anhui 230026 (China)
Fax: (+86) 551-360-3040
E-mail: shyu@ustc.edu.cn

Supporting information for this article is available on the WWW under http://www.chemeurj.org/ or from the author.

shows the time-dependent phase transformation and transition under the present solvothermal conditions. At the early stage of reaction, after about 2–3 h, only the hexagonal Se phase is observed (Figure 1a and Supporting Information Figure S1), which is in good agreement with the literature (JCPDS card number 06–0362).

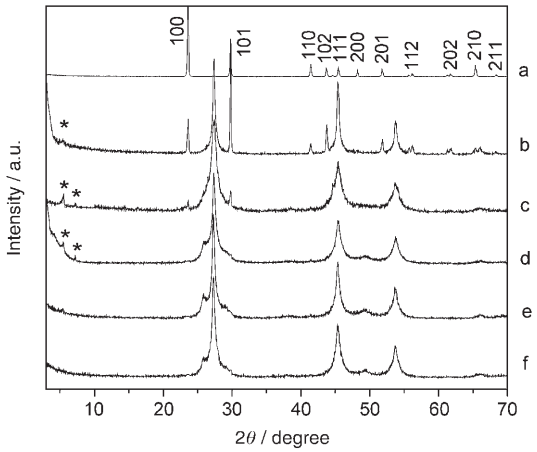

Figure 1. XRD patterns showing the time-dependent phase formation and transformation processes of the products prepared by the solvothermal reaction at 180 °C, with volume ratio V_{DETA}:V_{DIW} = 3:1. a) Pure Se 3 h, b) 4 h, c) 6 h, d) 12 h, e) 24 h, f) 5 d. *: ZnSe·$(DETA)_{0.5}$ phase.

After a reaction time of 4 h, the product is a mixture of cubic ZnSe (JCPDS card number 37–1463), hexagonal Se, and ZnSe·$(DETA)_{0.5}$ (Figure 1b). After 6 h, the amount of Se decreases and the product transforms gradually into a cubic ZnSe phase (Figure 1c). After 12 h, the product is a mixture that can be indexed as a ZnSe phase and a small amount of ZnSe·$(DETA)_{0.5}$ (Figure 1d), corresponding to a wurtzite ZnSe phase (JCPDS card number 15–0105)[11c] and a phase previously reported by Li and co-workers,[15d] respectively. After increasing the reaction time to 1–5 days, the ZnSe·$(DETA)_{0.5}$ phase disappears and a pure wurtzite ZnSe phase is obtained (Figure 1e,f).

Complex wurtzite ZnSe structures with high hierarchy: SEM images show that complex flowerlike wurtzite ZnSe structures are formed after 12 h (Figure 2a). These structures are composed of branched nanosheets. The magnified SEM images in Figure 2b–d indicate that each nanosheet is in fact made up of twinned nanosheets, and numerous nanofibers are growing on the surface of each single nanosheet. A small gap is observed within each nanosheet pair, as indicated by the white arrow in Figure 2b. The yield of these ZnSe complex microspheres can reach as high as 90 %.

Time-dependent shape evolution upon growth of complex ZnSe structures: The nucleation and growth processes of these microspheres and their intermediates were investigated by performing time-dependent experiments. SEM was used to examine the morphology of the products. After reaction for 2 h, irregular Se spheres with smooth surfaces and large diameters ranging from 3.5 to 5.5 μm were produced (Supporting Information Figure S2). After 3 h, Se spheres with rough surfaces and diameters ranging from 1.5 to 3.5 μm were observed (Figure 3). If the reaction is prolonged to 4 h, a black-yellow product composed of three phases is obtained (Figure 1b). The SEM images reveal two kinds of dominant morphologies; flowerlike ZnSe microspheres with rough surface structure, and Se spheres (Figure 4a). Magnified images of a single ZnSe microsphere show that its surface is very rough (Figure 4b). The HRTEM images in Figure 5a,b were taken from the fractural part of the nanosheets, and indicate that each nanosheet is composed of many nanoparticles with diameters ranging from 3 to 13 nm. The lattice-resolved HRTEM images in Figure 5a,b show that the spacing of the observed lattice planes is approximately 3.0 and 3.3 Å, which is consistent with the spacing for the (101) planes of hexagonal Se and the (111)

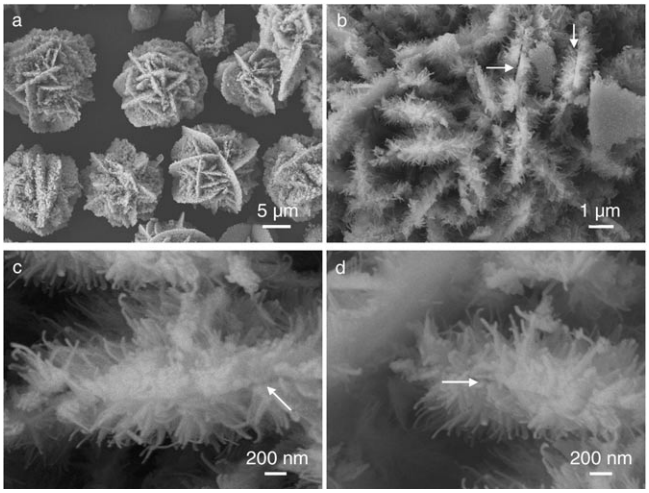

Figure 2. SEM images of the products prepared by the solvothermal reaction at 180 °C for 12 h, V_{DETA}:V_{DIW} = 3:1. a) A general-view image, b)–d) higher-magnification images showing the detailed surfaces of the fractural ZnSe microspheres. White arrows in b) indicate the twinned nanosheets with a gap in the middle part of the microsheet. White arrows in c) and d) indicate that the nanofibers are standing on the microsheets.

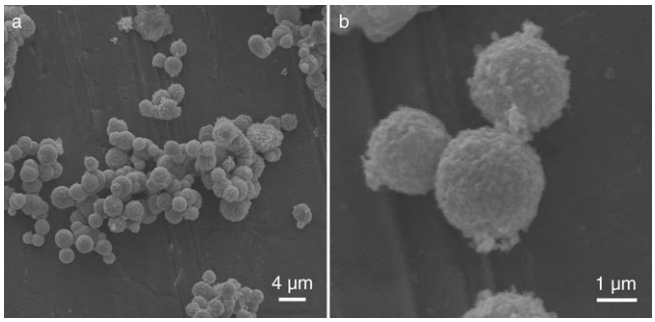

Figure 3. SEM images of the product prepared at 180 °C for 3 h, V_{DETA}:V_{DIW} = 3:1.

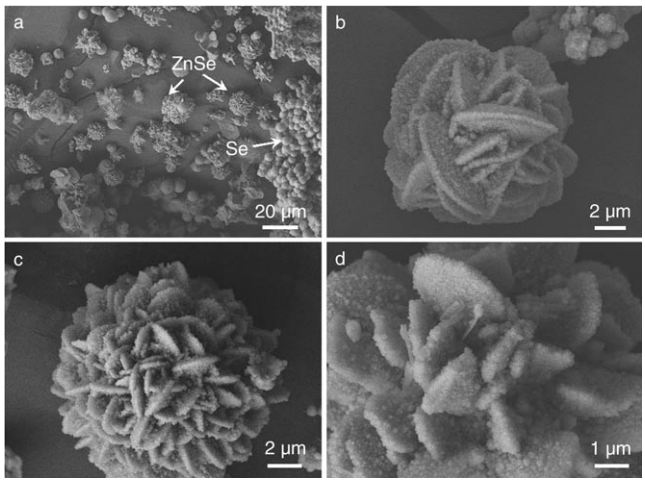

Figure 4. SEM images of the products prepared by a solvothermal reaction at 180 °C for 4 h, V_{DETA}:V_{DIW} = 3:1. a) A low-magnification image, b)–d) higher magnification images of the surface of the products. White arrows in a) indicate the single ZnSe microspheres.

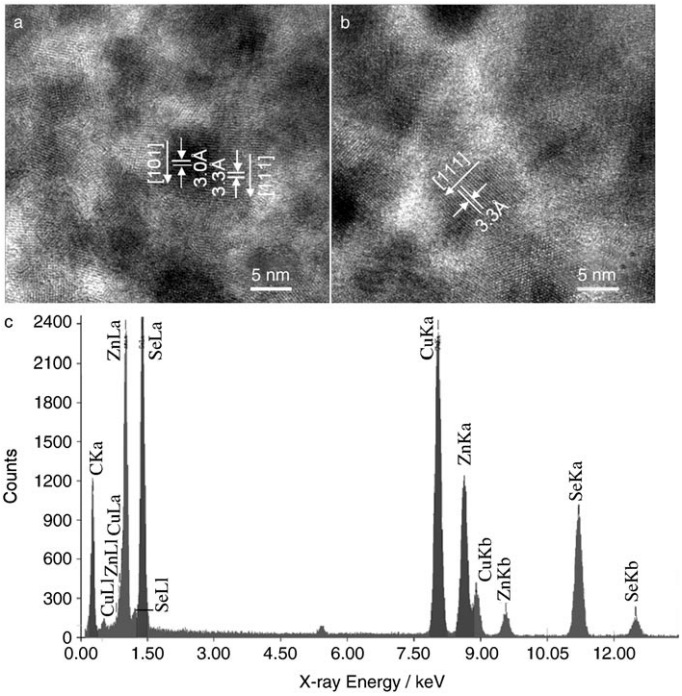

Figure 5. a), b) HRTEM images of nanosheets of the product prepared at 180 °C for 4 h, V_{DETA}:V_{DIW} = 3:1. c) The corresponding EDX spectra taken from the nanosheet shown in a). The Cu signals are due to the copper TEM grid.

planes of cubic ZnSe, respectively. The energy-dispersive X-ray (EDX) analysis of the local area of the sample prepared at 180 °C for 4 h shown in Figure 5c suggests that the atom ratio of Zn:Se is 1:12.7. This confirms that selenide is more abundant than zinc, and is also consistent with the XRD results shown in Figure 1b. The peaks of Cu and C originate from the Cu grids. Thus, the nanosheets are built from tiny nanoparticles, and these nanosheets tend to aggregate together and form branched flowerlike microspheres (Figure 4b–d).

Prolonging the reaction time results in a significant change in the morphology of the ZnSe microspheres. Figure 6 shows SEM images of the products that were obtained after the reaction proceeded for 6 h, 12 h, 24 h, and 5 d. These images clearly demonstrate the evolution of ZnSe nanostructures from balls of sheets to more complex flowerlike aggregates with a delicate surface structure. After 6 h, all the microspheres became fractal (Figure 6a and Supporting Information Figure S3). A certain specific distance is maintained between the pairs of twinning nanosheets because the charged nanosheets strongly repulse each other to neutralize the interface charges. The gap between two polar crystal faces could be due to a combination of Coulomb repulsion interactions, intermolecular forces, or Van der Waals attraction forces between two (001) polar surfaces. Recently, Wang et al. demonstrated that the polar nanowires/nanobelts can be self-assembled into more complex nanoarchitectures, such as ZnO nanorings, nanohelices, or nanosprings.[20] Their results show that the surface polarity adds an important parameter in controlling the shapes of ZnO nanostructures. Similarly, it is possible that the growth of nanostructures on the ZnSe nanosheets can be induced on polar surfaces.

The growth of the complex ZnSe microspheres was followed carefully. The surface of each nanosheet becomes coarser (Figure 4a), and many thin and short delicate nanofibers are formed. As the reaction time is extended to 12 h,

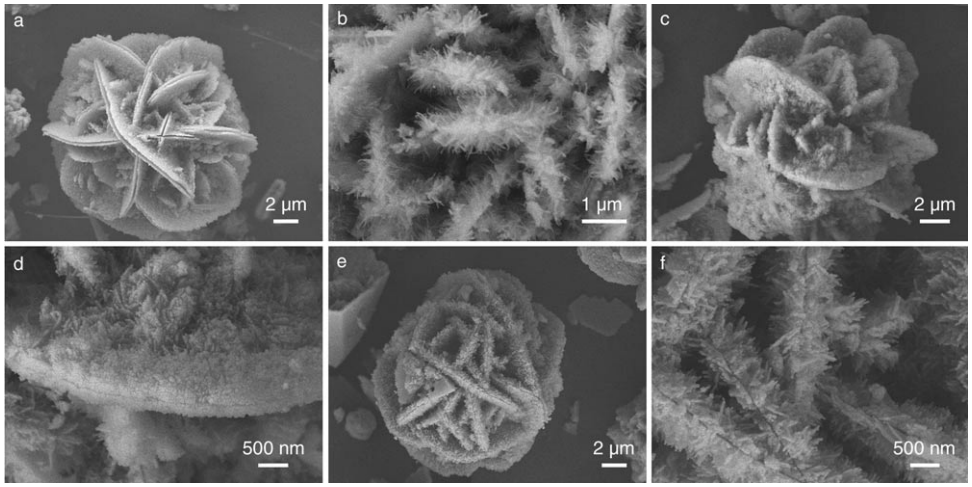

Figure 6. SEM images of the products prepared after different reaction times at 180 °C, V_{DETA}:V_{DIW} = 3:1. a) 6 h, b) 12 h, c), d) 24 h, e), f) 5 d. A typical spherical aggregate is composed of twinned nanosheets, as shown in a).

24 h, and 5 d, the fractal structure of the microspheres does not change, however, the surface structure of the microsheets changes dramatically. After 12 h, a hierarchical structure forms, in which long, flexible nanofibers are attached to the nanosheets (Figure 6b). Over the next 12 h, these nanofibers then tend to change gradually into nanosheets (Figure 6c,d), until the final hierarchal structure is formed, in which these newly formed nanosheets are standing on the surfaces of the initially formed nanosheets (Figure 6e,f).

If the volume ratio of deionized water (DIW) and DETA is greater or less than 3:1, the fractal ZnSe structure cannot form. If the ratio reaches 4:1 or 2.5:1, hollow ZnSe microspheres or $ZnSe(DETA)_{0.5}$ nanosheets develop, indicating that the volume ratio of DIW and DETA plays a crucial role in the formation of such complex ZnSe nanostructures. Under the same conditions, if the reaction temperature is lower than 180 °C, for example, 120 °C or 160 °C, the phase is not pure and a large amount of Se appeared. This indicates that at low temperatures, the basic thermodynamic and kinetic energy requirements to produce pure hexagonal ZnSe complex microspheres cannot be met.

Figure 7a,c show HRTEM images of nanofibers growing on the surface of the nanosheets that are also reported in Figure 2c,d. The selected-area electron-diffraction (SAED)

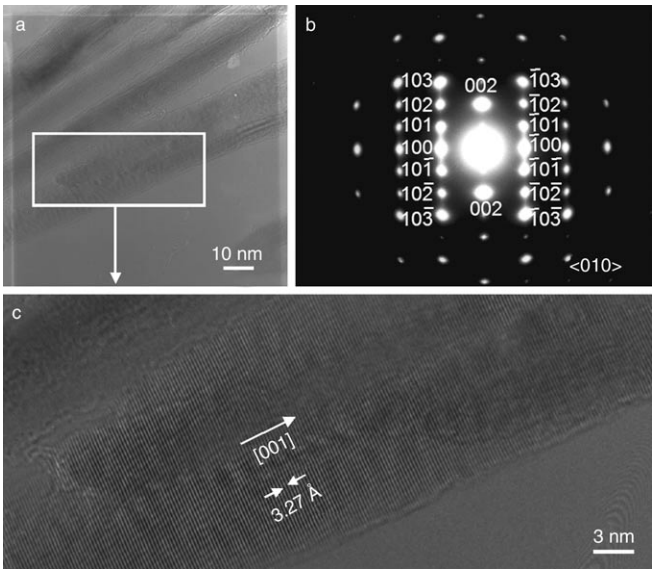

Figure 7. a), c) HRTEM images of nanofibers growing on the nanosheets prepared at 180 °C for 12 h. b) The corresponding electron diffraction pattern.

pattern confirmed that the nanofibers are single crystalline, and can be indexed as the [010] zone axis of the hexagonal ZnSe phase (Figure 7b). A lattice-resolved HRTEM image in Figure 7c indicates that the spacing of the observed lattice planes is approximately 3.27 Å, which is consistent with the spacing for the (002) planes of wurtzite ZnSe. The results suggest that the nanofibers grow preferentially along the *c* axis.

Composition analysis of complex ZnSe structures: The microspheres obtained at 180 °C for 12 h were characterized by using the X-ray photoelectron spectroscopy (XPS) technique (Figure 8). The binding energies of Se 3d and Zn $2p^3$ were identified at 55.05 and 1023.20 eV, respectively. The signals at 10.3 and 990.10 eV can be attributed to the binding energy of Zn 3p and the kinetic energy of Zn LMM. Notably, the signal of Zn $2p^3$, which is easily affected by the chemical environment, is stronger than that of Zn 3p. This result implies that the surface of the ZnSe obtained is not exposed to air, due to the good passivation of DETA. The Auger parameter, which is derived from the binding energy of Zn $2p^3$ and the kinetic energy of Zn LMM, is approximately 2011.60 eV, which is consistent with that of ZnSe. Quantitative analysis gives the atom ratio of Zn:Se as 1:1.20 and proves that the selenide content is greater than that of zinc. The signal at 400.95 eV can be attributed to N 1s, which originates from diethylenetriamine (DETA) adsorbing in the microspheres.

The FTIR spectra in Figure 9 show that the vibration bands of $-CH_2-$, $-NH_2$, C–N, and –NH belonging to DETA can be observed clearly, suggesting the existence of DETA in the product. Compared with the IR spectrum of pure DETA, the vibration band of C–N at 1126.84 cm^{-1} shifted toward a lower wavenumber (1060.17 cm^{-1}) in the microspheres, and –NH at 908.72 cm^{-1} and 698.53 cm^{-1} also changed and became almost invisible. Furthermore, the intensities for almost all vibration bands are weak and several bands are even missing.

Figure 10 shows a typical room-temperature Raman spectrum of the ZnSe microspheres. The Raman peaks at 204.21 and 250.80 cm^{-1} are attributed to the transverse optic (TO) and longitudinal optic (LO) phonon modes, respectively, of ZnSe. No vibration modes due to impurities are observed. From previous reports,[21] the LO phonon frequency of single-crystalline ZnSe film is 254 cm^{-1}, and that of single-crystal ZnSe is 255 cm^{-1} at room temperature. For ZnSe nanoparticles, the TO and LO phonon frequencies are 210 and 255 cm^{-1}, respectively, and both give a broad Raman peak due to the high surface-to-volume ratio of the structures.[21a,c,d,g,f] Both the LO and TO phonon peaks of the complex ZnSe structures are shifted toward lower frequency, which is probably due to the effects of special fine nanostructures.

Optical properties: The photoluminescence (PL) emission spectra of the products synthesized after different reaction times are shown in Figure 11. Figure 11a,b show strong narrow emission bands with maxima at 350 nm (3.55 eV), corresponding to a band-edge emission similar to that reported for cubic ZnSe nanoparticles synthesized by using a reverse-micellar approach.[22] In addition, a broad emission band centered at 372 nm (3.34 eV) (Figure 11a,b) is also similar to that observed for the sphalerite ZnSe nanocrystals or ZnSe quantum dots synthesized by using trioctylphosphine (TOPO) and hexadecylamine (HAD) capping reagents.[2,3,5,10c–e,3] Compared with the bulk band gap of the

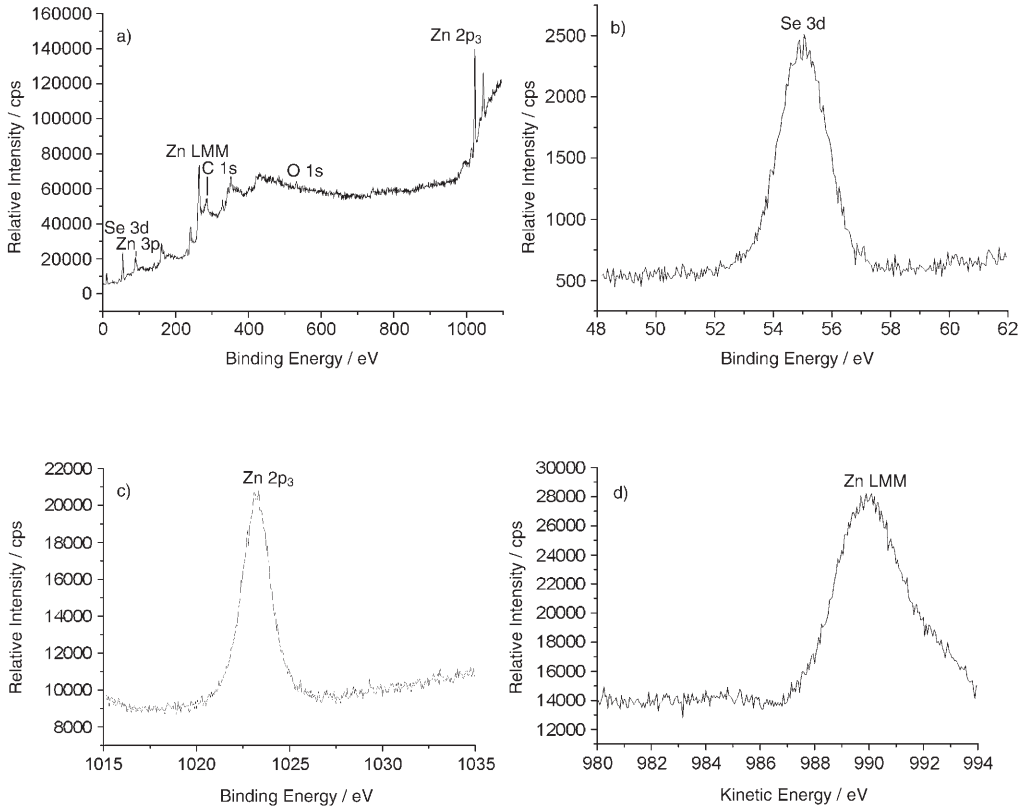

Figure 8. XPS spectra of ZnSe microspheres. a) Survey spectrum, b) Se 3d, c) Zn $2p^3$, d) Zn LMM.

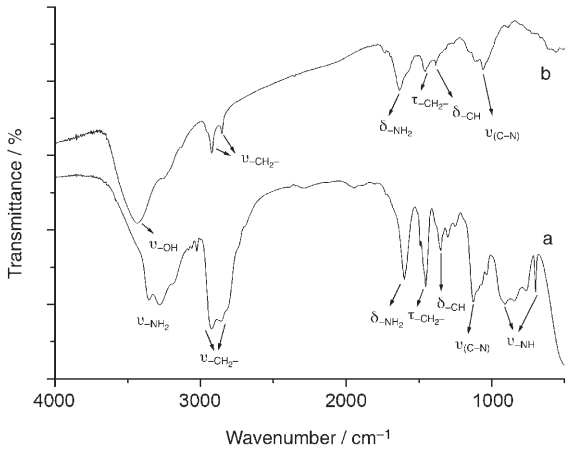

Figure 9. FTIR spectra of a) pure DETA and b) the products prepared at 180 °C for 12 h, V_{DIW}:V_{DETA} = 3:1.

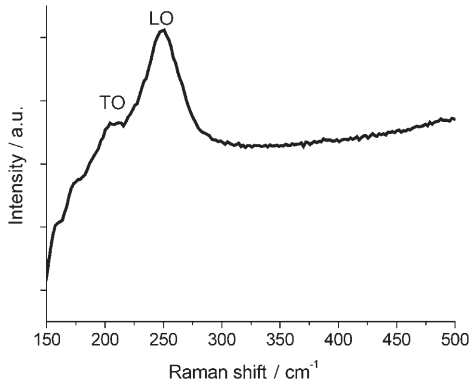

Figure 10. Room-temperature Raman spectrum of complex ZnSe nanostructures obtained at 180 °C for 12 h.

ZnSe, there is a large blue-shift in emission band.[2,3] The appearance of emission bands at 350 and 372 nm may be due to two size distributions in the samples shown in Figure 11a. During prolonged reactions, the emission band at 372 nm is weakened and finally disappears, as shown in Figure 11c,d. This is accompanied by the appearance of the strong and broad emission bands at 415 nm (2.99 eV), 435 nm (2.85 eV), and 460 nm (2.7 eV), which could be due to the increase in nanoparticle size. The emission band at 460 nm (2.70 eV) corresponds to the bulk band emission of ZnSe (Figure 11c).[24a,b] As the reaction time reached 48 h, the 350 nm emission band disappeared (Figure 11d), and as the reaction continued further, the emission band shifted toward a lower energy level of 540–700 nm. The lower-energy emissions of about 595 nm (2.09 eV) (Figure 11b), 592 nm (2.10 eV), and 606 nm (2.04 eV) (Figure 11e) were usually assigned to self-activated luminescence, probably as a result of some donor–acceptor pairs related to Zn-vacancy and interstitial states,[11a,12e,23] which are possible in the present case because the XPS data proves that the molar content of

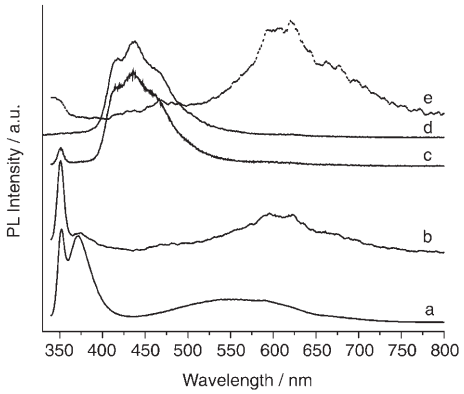

Figure 11. Photoluminescence (PL) emission spectra of the products obtained at 180 °C after different reaction times, $V_{DETA}:V_{DIW}=3:1$. a) 6 h, b) 12 h, c) 24 h, d) 48 h, e) 5 d. Excitation wavelength was 260 nm.

selenide is greater than that of zinc. In addition, such emissions at lower energy levels are usually attributed to doped ion emission for ZnSe crystals or thin films.[12e,24]

These results suggest that the optical properties of ZnSe nanostructures synthesized by the present approach in a binary solution are quite sensitive to the detailed reaction conditions. The origination of the different emission components achieved under different conditions warrants further investigation.

Conclusions

Complex ZnSe microspheres with high hierarchy that are composed of fractal nanosheets decorated with delicate wurtzite nanofibers can be grown easily by mild solvothermal reaction in a binary solution of diethylenetriamine (DETA) and water. Such complex structures display quantum-size effects and strong band-gap emission. Although the mechanism of formation of the ZnSe fractal structure is still unclear, it is apparent that the content of either the DETA template or water in such a binary solution plays a crucial role in the formation of these complex structures. This route is expected to afford various forms of ZnSe microstructures with complexity and special structural features. Furthermore, this approach could provide an effective strategy for tuning the electronic and optical properties of semiconductors, with special advantages over the traditional high-temperature approach, and could be extended to provide other semiconductor materials with unusual morphologies and structures.

Experimental Section

Materials and preparation: All chemicals were of analytical grade and were used as received without further purification. In a typical procedure, $ZnSO_4{\cdot}7H_2O$ (0.432 g, ~1.5 mmol) and Na_2SeO_3 (0.259 g, ~1.5 mmol) were added to a mixture of deionized water (DIW) and diethylenetriamine (DETA) with a volume ratio of 3:1. The mixed solution was then transferred to a Teflon-lined autoclave (at 80% of its total capacity of 50 mL). The autoclave was sealed and maintained at 180 °C for 12 h, and then cooled naturally to room temperature. After the reaction was completed, the solution was filtered, washed sequentially with deionized water and absolute ethanol, and dried in a vacuum at 80 °C for 6 h.

Characterization: XRD patterns of the products were obtained by using a Japan Rigaku DMax-γA rotation anode X-ray diffractometer equipped with graphite monochromatized $Cu_{K\alpha}$ radiation ($\lambda=1.54178$ Å). The SEM images were taken by using a field-emission scanning electron microscope (JEOL JSM-6700F, 15 kV). TEM photographs were taken by using a Hitachi Model H-800 transmission electron microscope at an accelerating voltage of 200 kV. HRTEM photographs and selected-area electron-diffraction (SAED) patterns were obtained by using a JEOL JEM 2011 microscope at an accelerating voltage of 200 kV. Energy-dispersive X-ray (EDX) analysis was performed by using an EDAX detector installed on the same HRTEM. The X-ray photoelectron spectra (XPS) were collected by using an ESCALab MKII X-ray photoelectron spectrometer with nonmonochromatized $Mg_{K\alpha}$ X-ray as the excitation source. FTIR spectra were measured by using a Bruker Vector-22 FTIR spectrometer from 4000 to 400 cm^{-1} at room temperature. Raman scattering spectra were recorded by using a Renishaw System 2000 spectrometer using the 514 nm line of Ar^+ for excitation. Photoluminescence (PL) spectra were recorded by using a Fluorolog3-TAU-P at room temperature.

Acknowledgements

S.-H.Y. thanks the funding support from the Centurial Program of the Chinese Academy of Sciences, the National Science Foundation of China (nos. 20325104, 20321101, 50372065), and the Scientific Research Foundation for the Returned Overseas Chinese Scholars, State Education Ministry. We thank Dr. Jun-Qing Hu, Advanced Materials Laboratory and Nanomaterials Laboratory, National Institute for Materials Science (NIMS), for his generous support in the HRTEM analysis presented in this paper. We also thank the referee of this paper for his valuable suggestions at the revision stage.

[1] M. A. Haase, J. Qiu, J. M. DePuydt, H. Cheng, *Appl. Phys. Lett.* **1991**, *59*, 1272.
[2] M. A. Hines, P. Guyot-Sionnest, *J. Phys. Chem. B* **1998**, *102*, 3655.
[3] Y. W. Jun, J. E. Koo, J. Cheon, *Chem. Commun.* **2000**, 1243.
[4] F. T. Quinlan, J. Kuther, W. Tremel, W. Knoll, S. Risbud, P. Stroeve, *Langmuir* **2000**, *16*, 4049.
[5] M. A. Malik, N. Revaprasadu, P. O'Brien, *Chem. Mater.* **2001**, *13*, 913.
[6] a) M. Y. Chern, H. M. Lin, C. C. Fang, J. C. Fan, Y. F. Chen, *Appl. Phys. Lett.* **1995**, *67*, 1390; b) J. Wang, X. H. Liu, Z. S. Li, R. Z. Su, Z. Ling, W. Z. Cai, X. Y. Hou, X. Wang, *Appl. Phys. Lett.* **1995**, *67*, 2043; c) M. S. Koo, T. J. Kim, M. S. Lee, M. S. Oh, Y. D. Kim, S. D. Yoo, D. E. Aspnes, B. T. Jonker, *Appl. Phys. Lett.* **2000**, *77*, 3364; d) G. Riveros, J. F. Guillemoles, D. Lincot, H. Gomez Meier, M. Froment, M. C. Bernard, R. Cortes, *Adv. Mater.* **2002**, *14*, 1286.
[7] a) M. C. H. Liao, Y. H. Chang, Y. F. Chen, J. W. Hsu, J. M. Lin, W. C. Chou, *Appl. Phys. Lett.* **1997**, *70*, 2256; b) C. A. Smith, H. W. H. Lee, V. J. Leppert, S. H. Risbud, *Appl. Phys. Lett.* **1999**, *75*, 1688; c) T. Tawara, S. Tanaka, H. Kumano, I. Suemune, *Appl. Phys. Lett.* **1999**, *75*, 235; d) G. von Freymann, D. Lüerßen, C. Rabenstein, M. Mikolaiczyk, H. Richter, H. Kalt, T. Schimmel, M. Wegener, K. Okhawa, D. Hommel, *Appl. Phys. Lett.* **2000**, *76*, 203; e) H. Zhao, S. Moehl, H. Kalt, *Appl. Phys. Lett.* **2002**, *80*, 1391; f) H. Zhao, S. Moehl, H. Kalt, *Appl. Phys. Lett.* **2002**, *81*, 2794; g) H. S. Chen, B. Lo, J. Y. Hwang, G. Y. Chang, C. M. Chen, S. J. Tasi, S. J. Wang, *J. Phys. Chem. B* **2004**, *108*, 17119.
[8] E. Tournié, C. Morhain, G. Neu, J. P. Faurie, R. Triboulet, J. O. Ndap, *Appl. Phys. Lett.* **1996**, *68*, 1356.

[9] a) E. Monroy, F. Vigué, F. Calle, J. I. Izpura, E. Muñoz, J. P. Faurie, *Appl. Phys. Lett.* **2000**, *77*, 2761; b) J. F. Holzman, F. E. Vermeulen, S. E. Irvine, A. Y. Elezzabi, *Appl. Phys. Lett.* **2002**, *81*, 2294; c) J. Nürnberger, W. Faschinger, R. Schmitt, M. Korn, M. Ehinger, G. Landwehr, *Appl. Phys. Lett.* **1997**, *70*, 1281; d) D. Albert, J. Nürnberger, V. Hock, M. Ehinger, W. Faschinger, G. Landwehr, *Appl. Phys. Lett.* **1999**, *74*, 1957; e) D. A. Gaul, W. S. Rees, *Adv. Mater.* **2000**, *12*, 935; f) S. T. Selvan, C. Bullen, M. Ashokkumar, P. Mulvaney, *Adv. Mater.* **2001**, *13*, 985.

[10] a) D. J. Norris, N. Yao, F. T. Charnock, T. A. Kennedy, *Nano Lett.* **2001**, *1*, 3; b) G. N. Karanikolos, P. Alexandridis, G. Itskos, A. Petrou, T. J. Mountziaris, *Langmuir* **2004**, *20*, 550; c) A. Shavel, N. Gaponik, A. Eychmuller, *J. Phys. Chem. B* **2004**, *108*, 5905; d) L. S. Li, N. Pradhan, Y. Wang, X. Peng, *Nano Lett.* **2004**, *4*, 2261; e) S. L. Cumberland, K. M. Hanif, A. Javier, G. A. Khitrov, G. F. Strouse, S. M. Woessner, C. S. Yun, *Chem. Mater.* **2002**, *14*, 1576.

[11] a) J. Q. Hu, Y. Bando, D. Golberg, *Small* **2005**, *1*, 95; b) M. Kazes, D. Y. Lewis, Y. Ebenstein, T. Mokari, U. Banin, *Adv. Mater.* **2002**, *14*, 317; c) R. T. Lv, C. B. Cao, H. Z. Zhai, D. Z. Wang, S. Y. Liu, H. S. Zhu, *Solid State Commun.* **2004**, *130*, 241.

[12] a) Q. Li, X. Gong, C. Wang, J. Wang, K. Ip, S. Hark, *Adv. Mater.* **2004**, *16*, 1436; b) X. T. Zhang, Z. Liu, Y. P. Leung, Q. Li, S. K. Hark, *Appl. Phys. Lett.* **2003**, *83*, 5533; c) Y. F. Chan, X. F. Duan, S. K. Chan, I. K. Sou, X. X. Zhang, N. Wang, *Appl. Phys. Lett.* **2003**, *83*, 2665; d) X. T. Zhang, K. M. Ip, Z. Liu, Y. P. Leung, Q. Li, S. K. Hark, *Appl. Phys. Lett.* **2004**, *84*, 2641; e) Y. Jiang, X. M. Meng, W. C. Yiu, J. Liu, J. X. Ding, C. S. Lee, S. T. Lee, *J. Phys. Chem. B* **2004**, *108*, 2784.

[13] Q. Peng, Y. J. Dong, Y. D. Li, *Angew. Chem.* **2003**, *115*, 3135; *Angew. Chem. Int. Ed.* **2003**, *42*, 3027.

[14] a) S. H. Yu, Y. S. Wu, J. Yang, Z. H. Han, Y. Xie, Y. T. Qian, X. M. Liu, *Chem. Mater.* **1998**, *10*, 2309; b) J. Yang, C. Xue, S. H. Yu, J. H. Zeng, Y. T. Qian, *Angew. Chem.* **2002**, *114*, 4891; *Angew. Chem. Int. Ed.* **2002**, *41*, 4697.

[15] a) X. Y. Huang, J. Li, H. X. Fu, *J. Am. Chem. Soc.* **2000**, *122*, 8789; b) X. Y. Huang, H. R. Heulings, V. Le, J. Li, *Chem. Mater.* **2001**, *13*, 3754; c) H. R. Heulings, X. Huang, J. Li, T. Yuen, C. L. Lin, *Nano Lett.* **2001**, *1*, 521; d) X. Y. Huang, J. Li, Y. Zhang, A. Mascarenhas, *J. Am. Chem. Soc.* **2003**, *125*, 7049.

[16] S. H. Yu, M. Yoshimura, *Adv. Mater.* **2002**, *14*, 296.

[17] a) Z. X. Deng, C. Wang, X. M. Sun, Y. D. Li, *Inorg. Chem.* **2002**, *41*, 869; b) Z. X. Deng, L. B. Li, Y. D. Li, *Inorg. Chem.* **2003**, *42*, 2331.

[18] W. T. Yao, S. H. Yu, L. Pan, J. Li, Q. S. Wu, L. Zhang, J. Jiang, *Small* **2005**, *1*, 320.

[19] W. T. Yao, S. H. Yu, X. Y. Huang, J. Jiang, L. Q. Zhao, L. Pang, J. Li, *Adv. Mater.* **2005**, *17*, 2799.

[20] a) Z. L. Wang, *J. Mater. Chem.* **2005**, *15*, 1021; b) X. Y. Kong, Y. Ding, R. Yang, Z. L. Wang, *Science* **2004**, *303*, 1348; c) C. Ma, Y. Ding, D. Moore, X. D. Wang, Z. L. Wang, *J. Am. Chem. Soc.* **2004**, *126*, 708; d) Z. L. Wang, L. Wang, X. Y. Kong, Y. Ding, P. X. Gao, W. L. Hughes, R. Yang, Y. Zhang, *Adv. Funct. Mater.* **2004**, *14*, 943; e) R. Yang, Y. Ding, Z. L. Wang, *Nano Lett.* **2004**, *4*, 1309; f) X. Y. Kong, Z. L. Wang, *Appl. Phys. Lett.* **2004**, *84*, 975; g) P. X. Gao, Z. L. Wang, *Appl. Phys. Lett.* **2004**, *84*, 2883; h) D. Moore, C. Ronning, C. Ma, Z. L. Wang, *Chem. Phys. Lett.* **2004**, *385*, 8; i) X. Y. Kong, Z. L. Wang, *Nano Lett.* **2003**, *3*, 1625; j) Z. L. Wang, X. Y. Kong, J. M. Zuo, *Phys. Rev. Lett.* **2003**, *91*, 185502.

[21] a) D. Sarigiannis, J. D. Peck, G. Kioseoglou, A. Petrou, T. J. Mountziaris, *Appl. Phys. Lett.* **2002**, *80*, 4024; b) D. Sarigiannis, J. D. Peck, T. J. Mountziaris, G. Kioseoglou, A. Petrou, *Mater. Res. Soc. Symp. Proc.* **2000**, *616*, 41; c) B. Schreder, A. Materny, W. Kiefer, G. Bacher, A. Forchel, G. Landwehr, *J. Raman Spectrosc.* **2000**, *31*, 959; d) G. Lermann, T. Bischof, A. Materny, W. Kiefer, T. Kummell, G. Bacher, A. Forchel, G. Landwehr, *J. Appl. Phys.* **1997**, *81*, 1446; e) T. J. Mountaiaris, J. D. Peck, S. Stoltz, W. Y. Yu, A. Petrou, P. G. Mattocks, *Appl. Phys. Lett.* **1996**, *68*, 2270; f) C. L. Mak, R. Sooryakumar, B. T. Jonker, G. A. Prinz, *Phys. Rev. B* **1992**, *45*, 3344.

[22] F. T. Quinlan, J. Kuther, W. Tremel, W. Knoll, S. Risbud, P. Stroeve, *Langmuir* **2000**, *16*, 4049.

[23] a) J. A. Garcia, A. Remon, A. Zubiaga, V. M. Sanjose, C. M. Tomas, *Phys. Status Solidi A* **2002**, *194*, 338; b) J. F. Suyver, S. F. Wuister, J. J. Kelly, A. Meijerink, *Phys. Chem. Chem. Phys.* **2000**, *2*, 5445; c) *Phosphor Handbook* (Eds.: S. Shionoya, W. M. Yen), CRC Press, Washington, DC, **1998**, Chapter 3, pp. 238–248.

[24] a) M. Klude, D. Hommel, *Appl. Phys. Lett.* **2001**, *79*, 2523; b) J. Mazher, S. Badwe, R. Sengar, D. Gupta, R. K. Pandey, *Phys. E* **2003**, *16*, 209; c) T. J. Norman, D. Magana, T. Wilson, C. Burns, J. Z. Zhang, D. Cao, F. Bridges, *J. Phys. Chem. B* **2003**, *107*, 6309.

Received: July 18, 2005
Published online: January 13, 2006

